



WAVEGUIDES WITH PERIODIC UNDULATIONS INSPIRED BY DSP WINDOWING

M. A. HAWWA

Seagate Technology, Advanced Platform Development Group, 5898 Condor Drive,
Moorpark, CA 93021, U.S.A.

(Received 26 July 1996, and in final form 5 August 1997)

1. INTRODUCTION

This study is to investigate filter characteristics of periodic waveguides having non-uniform periodicities. Such periodicities can be provided in the form of taper functions, similar in nature to the window functions in the area of digital signal processing.

Previous works on acoustic wave propagation in ducts with periodic walls include the works by Nayfeh [1, 2] who studied the interaction of two modes in a two-dimensional hard-walled duct with sinusoidal walls, without and with mean flow. The interaction of two as well as three modes in a cylindrical hard-walled duct having generally weak undulations was considered by Nayfeh and Kandil [3]. A coupled-mode analysis of acoustic waves in a rectangular duct with sinusoidal undulations was performed by Nusayr [4]. An analysis of the banded structure of the dispersion spectrum of the modes of a cylindrical hard-walled duct having a sinusoidally varying cross-section was done by Bostrom [5]. The propagating of acoustic waves at the junction between a periodically undulated section of a cylindrical duct and straight ducts was investigated by Lundqvist and Bostrom [6]. The restriction of axial inversion symmetry and reciprocity on the allowed Bloch wave solution in a periodic waveguide was investigated by Bradley [7]. Recently, a design of single-mode as well as multi-mode acoustic silencers utilizing periodic undulations was put forward by Hawwa *et al.* [8].

All of the above references concentrated on periodic undulations with uniform amplitudes. There is a possibility, however, of employing tapered periodic undulations in a similar fashion to using a suitable window (weighting) function for the design of an enhanced digital filter.

In digital filter design, windows are utilized as weighting functions to smooth out the sidelobe ripples and the overshoots (Gibbs phenomenon) in the original frequency response. A response with low sidelobe levels is mainly desirable for two purposes: (1) the convergence of Fourier series in the vicinity of discontinuities is improved for windowed digital filters. (2) If the sidelobe level of the response is too high, the main lobe of a weak signal may be obscured by the sidelobe from the strong signal. The first windows used for these purposes were an *ad hoc* type such as those of Bartlett, Blackman, Hamming, and Hanning. Another family of windows with adjustable parameters were then suggested such as Kaiser's window, for which the ratio of the main lobe energy to the sidelobe energy is maximized. The choice of the window can play an important role in determining the quality of the digital filter design. For a detailed treatment of the subject, the reader is referred to the books by Rabiner and Gold [9] and Oppenheim and Schacter [10].

In this paper, the design of wave filters using tapered undulations inspired by the DSP window functions is presented. A circular cylindrical duct with a non-uniformly periodic rigid wall is studied as a basic example. By assuming small-amplitude wall undulations,

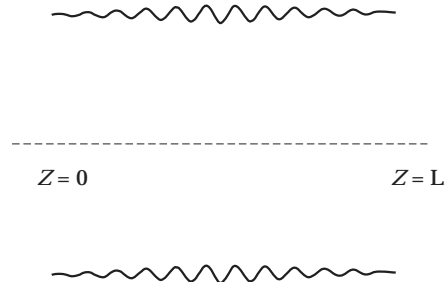


Figure 1. Waveguide with taper walls.

the perturbation method of multiple scales can be used to analyze the stopband interaction of the propagating acoustic modes with the wall of the duct when the Bragg resonance condition occurs. This leads to the coupled-mode equations with variable coefficients, which are provided with relevant boundary conditions to constitute a two-point boundary value problem. The missing boundary conditions are found numerically using the fundamental matrix method. The filter response is calculated in terms of the reflection coefficient.

2. PROBLEM FORMULATION

The propagation of time-harmonic acoustic waves in the rigid circular cylindrical duct shown in Figure 1 is considered. The radius of the duct varies in the region $z = [0, L]$

TABLE 1
Taper functions

Taper functions	DSP window
$T(Z_1) = 1 - (Z_1 - L/2)/(L/2) $	Bartlett
$T(Z_1) = 0.42 - 0.5 \cos(2\pi Z_1/L) + 0.08 \cos(4\pi Z_1/L)$	Blackman
$T(Z_1) = 0.54 - 0.46 \cos(2\pi Z_1/L)$	Hamming
$T(Z_1) = 0.5 - 0.5 \cos(2\pi Z_1/L)$	Hanning
$T(Z_1) = I_0(\beta((L/2)^2 - (Z_1 - L/2)^2)^{1/2})/I_0(\beta(L/2)^2)$	Kaiser
$T(Z_1) = 1 - ((Z_1 - L/2)/(L/2))^2$	Welsh
$T(Z_1) = 1$	Rectangular

TABLE 2
Summary of results

Taper function	Peak ripple (dB)	Transition bandwidth (Hz)
Bartlett	-32	75
Blackman	-110	215
Hamming	-72	120
Hanning	-61	95
Kaiser ($\beta = 1$)	-33	45
Kaiser ($\beta = 2$)	-92	145
Kaiser ($\beta = 3$)	-146	280
Welsh	-43	35
Rectangular	-12	5

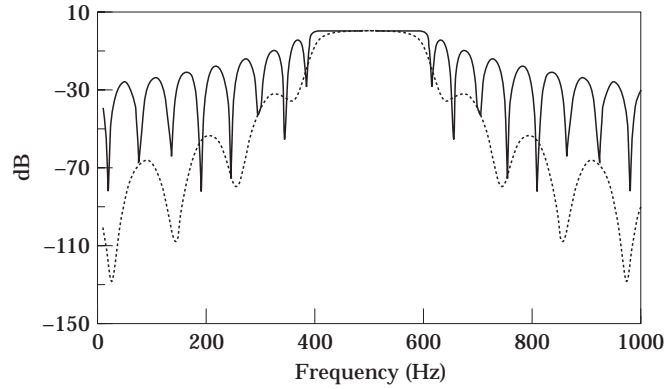


Figure 2. Filter response (Bartlett taper function, dotted).

according to the distortion function

$$\hat{r}(\hat{z}) = \hat{a}[1 + \varepsilon T(\hat{z}) \sin \hat{k}_w \hat{z}], \quad (1)$$

where \hat{a} is the average radius in the distorted region, which is also equal to the radius of the uniform section of the duct; \hat{k}_w is the wavenumbers of the wall undulation, $\varepsilon \ll 1$ is a dimensionless parameter equal to the ratio of the amplitude of the wall undulation to \hat{a} , and $T(\hat{z})$ is a slowly varying taper function, which acts as weighting function. When $T(\hat{z}) = 1$, the problem reduces to that of a duct with uniform undulations.

In order to perform a perturbation analysis, the problem using \hat{a} as a spatial reference quantity is normalized. Then, the governing equation of acoustic waves in the duct is given by

$$\left[\left(\frac{1}{r} \frac{\partial}{\partial r} \left(r \frac{\partial}{\partial r} \right) + \frac{1}{r^2} \frac{\partial^2}{\partial \theta^2} + \frac{\partial^2}{\partial z^2} \right) + k^2 \right] p = 0, \quad (2)$$

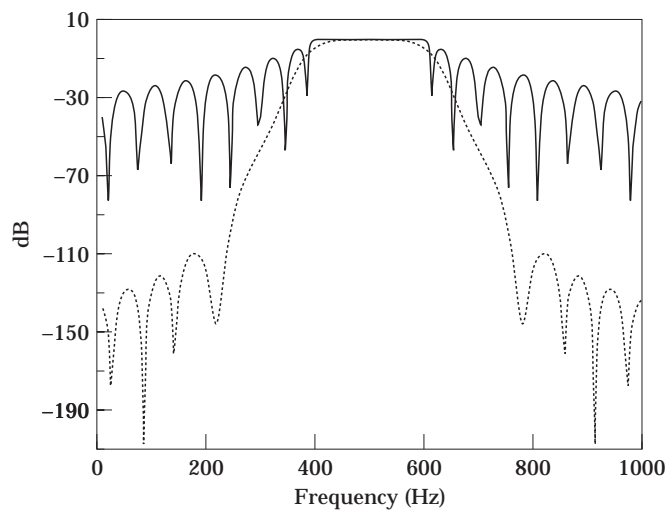


Figure 3. Filter response (Blackman taper function, dotted).

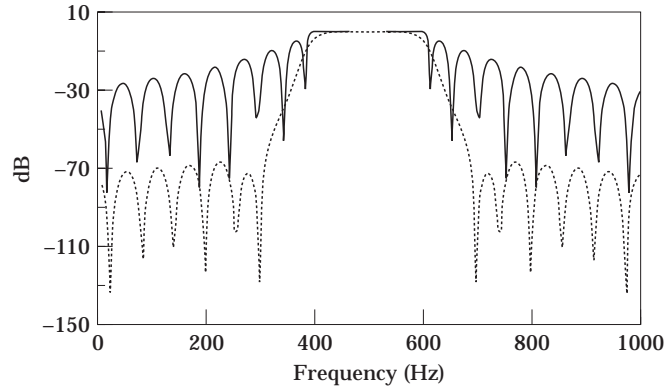


Figure 4. Filter response (Hamming taper function, dotted).

where p is the acoustic pressure inside the duct, $k = \omega \hat{a}/c$ is the nondimensional free acoustic wavenumber, where ω is the circular frequency and c is the speed of sound.

The governing equation is subject to the boundary condition of vanishing velocity component normal to the duct wall, hence

$$\nabla p \cdot \mathbf{n} = \frac{\partial p}{\partial r} n_r + \frac{\partial p}{\partial z} n_z = 0, \quad \text{at } r = 1 + \varepsilon T(z) \sin k_w z; \quad (3)$$

n_r and n_z are the r - and z - components of the local outward-pointing unit normal, respectively.

The system of equations (2) and (3) will be solved when the following resonance condition is satisfied:

$$2k_n \approx k_w. \quad (4)$$

Under this condition, a solution in the form of a straightforward first order asymptotic expansion is found to break down. It is known in the literature as Bragg resonance, which indicates that the incident and the reflected n th modes are coupled by the periodic

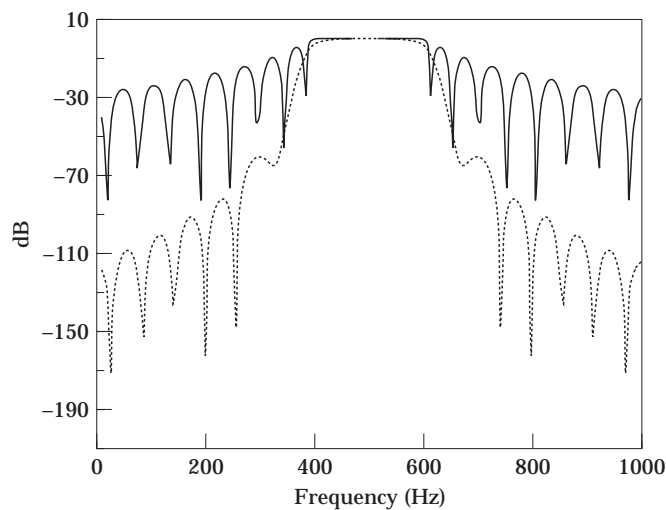


Figure 5. Filter response (Hanning taper function, dotted).

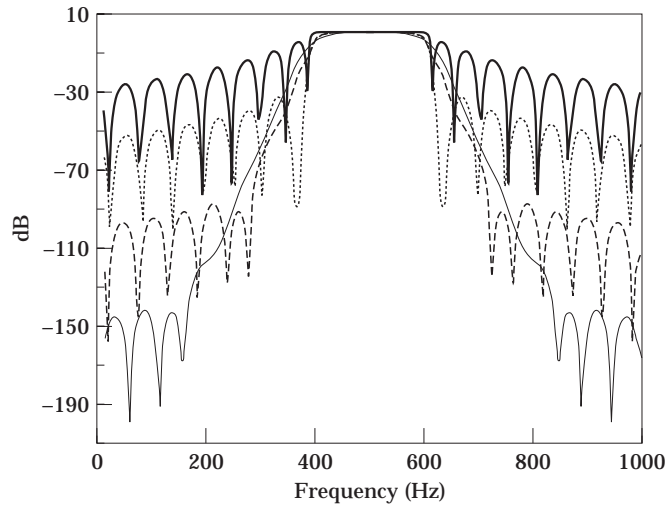


Figure 6. Filter response (Kaiser taper function); $\beta = 1$, dotted; $\beta = 2$, dashed; $\beta = 3$; solid.

undulation. To quantitatively evaluate the nearness to resonance, a detuning parameter $\sigma = \mathcal{O}(1)$ is used as a measure such that

$$2k_n + \varepsilon\sigma = k_w. \quad (5)$$

In the next section a uniform solution, valid around the resonance condition, is obtained using the method of multiple scales [11].

3. MULTIPLE SCALES FORMULATION

Using the method of multiple scales, one seeks a first order asymptotic expansion for p in powers of ε in the form

$$p(r, z) = p_0(r, Z_0, Z_1) + \varepsilon p_1(r, Z_0, Z_1) + \cdots, \quad (6)$$

where $Z_0 = z$ is a short scale of the order of the wavelength in the duct and $Z_1 = \varepsilon z$ is a long scale characterizing the amplitude and phase modulations due to the wall undulation.

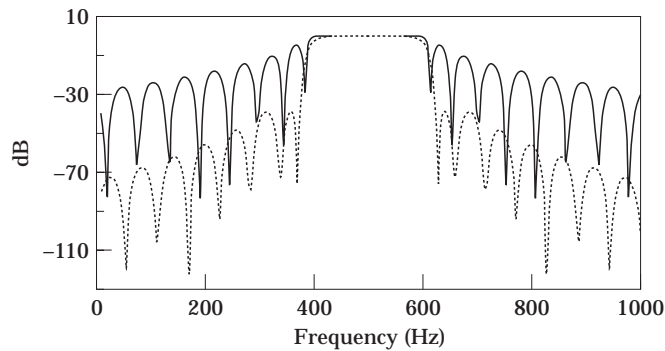


Figure 7. Filter response (Welsh taper function, dotted).

Using the chain rule, one can write the derivatives with respect to z in terms of Z_0 and Z_1 as

$$\frac{\partial}{\partial z} = \frac{\partial}{\partial Z_0} + \varepsilon \frac{\partial}{\partial Z_1} + \cdots, \quad \frac{\partial^2}{\partial z^2} = \frac{\partial^2}{\partial Z_0^2} + 2\varepsilon \frac{\partial^2}{\partial Z_0 \partial Z_1} + \cdots \quad (7, 8)$$

Substituting equations (6–8) into equations (2) and (3), expanding p at $r = 1 + \varepsilon T(Z_1) \sin k_w Z_0$ in a Taylor series around $r = 1$, and equating coefficients of equal powers of ε on both sides, one obtains for the zeroth order problem,

$$\left[\left(\frac{1}{r} \frac{\partial}{\partial r} \left(r \frac{\partial}{\partial r} \right) + \frac{1}{r^2} \frac{\partial^2}{\partial \theta^2} + \frac{\partial^2}{\partial Z_0^2} \right) + k^2 \right] p_0 = 0, \quad (9)$$

$$\partial p_0 / \partial r = 0, \quad \text{at } r = 1, \quad (10)$$

and for the first order problem,

$$\left[\left(\frac{1}{r} \frac{\partial}{\partial r} \left(r \frac{\partial}{\partial r} \right) + \frac{1}{r^2} \frac{\partial^2}{\partial \theta^2} + \frac{\partial^2}{\partial Z_0^2} \right) + k^2 \right] p_1 = -2 \frac{\partial^2 p_0}{\partial Z_0 \partial Z_1}, \quad (11)$$

$$\frac{\partial p_1}{\partial r} = -T(Z_1) \left[\sin k_w Z_0 \frac{\partial^2 p_0}{\partial r^2} - k_w \cos k_w Z_0 \frac{\partial p_0}{\partial Z_0} \right], \quad \text{at } r = 1. \quad (12)$$

One seeks a solution of equations (9) and (10) in the form of a linear combination of incident and reflected modes,

$$p_0 = \sum_{m,n} J_m(\gamma_{mn} r) [A_n^+(Z_1) e^{i(k_n Z_0 + m\theta)} + A_n^-(Z_1) e^{-i(k_n Z_0 - m\theta)}], \quad (13)$$

where the superscript $+$ and $-$ indicate incident and reflected modes, respectively. The axial wavenumber $k_n^2 = k^2 - \gamma_{mn}^2$, where γ_{mn} is a solution of the dispersion relation of the duct modes, $J_m(\gamma_{mn}) = 0$. The amplitudes A_n^\mp will be determined from the solvability condition at the next level of approximation. In order to determine this condition, one seeks a particular solution for p_1 in the form

$$p_1 = \sum_{m,n} [B_n^+(r) e^{i(k_n Z_0 + m\theta)} + B_n^-(r) e^{-i(k_n Z_0 - m\theta)}]. \quad (14)$$

By substituting equations (13) and (14) into the first order problem (11) and (12), and equating the coefficients of $\exp(\mp i k_n Z_0)$ on both sides, one obtains

$$\left[\frac{1}{r} \frac{\partial}{\partial r} \left(r \frac{\partial}{\partial r} \right) + \left(\gamma_{mn}^2 - \frac{m^2}{r^2} \right) \right] B_n^\mp = \pm 2i k_n \frac{\partial A_n^\mp}{\partial Z_1} J_m(\gamma_{mn} r), \quad (15)$$

$$\frac{\partial B_n^\mp}{\partial r} (1) = \mp \frac{i}{2} T(Z_1) [\gamma_{mn}^2 J_m''(\gamma_{mn}) - k_w k_n J_m(\gamma_{mn})] A_n^\pm e^{\pm i \sigma Z_1}. \quad (16)$$

Since the homogeneous first order problem has a non-trivial solution, the inhomogeneous first order problem has a solution if, and only if, a solvability condition is satisfied [13]. To determine this condition, one multiplies equation (15) by $r J_1(\gamma_{mn} r)$ and

integrates by parts from $r = 0$ to $r = 1$, and invoke equation (5). This leads to the coupled-mode equations

$$\frac{d}{dZ_1} \begin{Bmatrix} A_n^+ \\ A_n^- \end{Bmatrix} = \begin{bmatrix} 0 & T(Z_1)C_{mn} e^{-i\sigma Z_1} \\ T(Z_1)C_{mn} e^{i\sigma Z_1} & 0 \end{bmatrix} \begin{Bmatrix} A_n^+ \\ A_n^- \end{Bmatrix}, \quad (17)$$

where

$$C_{mn} = \frac{-1}{k_n} \left(\frac{\gamma_{mn}^2}{\gamma_{mn}^2 - m^2} \right) \left[\gamma_{mn}^2 \frac{J_m''(\gamma_{mn})}{J_m(\gamma_{mn})} - k_w k_n \right].$$

The coupled mode equations (17) form a first order ordinary differential equations with variable coefficients. Without loss of generality, end conditions at $Z_1 = 0$ and $Z_1 = l$ are assumed to be

$$A_n^+(0) = 1, \quad A_n^-(l) = 0, \quad (18)$$

where the first condition represents an excitation amplitude of the incident mode, and the second condition indicates an anechoic termination at $Z_1 \rightarrow \infty$.

In order to calculate the filter response of the duct, the two-point boundary value problem defined by equations (17) and (18) is solved numerically by employing the fundamental matrix method [12].

Before presenting numerical examples, the range of validity of the multiple-scales first order approximation is investigated. This can be done by extending the multiple-scale solution to second order in ε and neglecting the self interaction term. The same conclusion could be reached, however, if one specifies a threshold on the values of the detuning parameter, σ , since it is a measure of the nearness to resonance. If equation (5) is rewritten in the form $1 = k_w/2k_n - \varepsilon(\sigma/2k_n)$, one realizes that the quantity $\sigma/2k_n$ should be of the order of unity. Hence, an upper limit may be put on σ as: $-2k_n * \mathcal{O}(1) < \sigma < 2k_n * \mathcal{O}(1)$. By letting $|\sigma/2k| < 5$, for example, the range of validity of the first order perturbation expansion is such that $-10k < \sigma < 10k$. Hence, values of σ should be within this range.

4. NUMERICAL EXAMPLES

One takes a circular cylindrical duct with $\hat{a} = 0.1$ m as an example. Assume that the duct contains ambient air, in which $c = 343$ m/s. From the dispersion relation, one can show that at a frequency of 500 Hz only the plane wave can propagate and other modes are evanescent. In order to eliminate the propagating wave at 500 Hz, periodic wall undulations are designed having a wavenumber that is equal to twice the wavenumber k_n at this frequency, i.e., $k_w = 2 \times 0.916$, which corresponds to a wavelength $\lambda = 0.343$ m. The amplitude-related parameter, ε , and the length of the periodic section, l , are chosen to be 0.1 and 10λ , respectively.

Six types of taper functions are applied to the above described wall undulations. They are tabulated with the corresponding DSP windows as shown in Table 1. Note that the case of a uniformly undulated duct is obtained as a special case in the present analysis by letting $T(Z_1) = 1$. This corresponds to a window of the rectangular type.

The filter responses of the tapered silencers are depicted in Figures 2–7 and are compared to that of the uniformly undulated one. All of the taper functions are noticed to have the same effects, with different degrees of influence. These are: (1) realizing larger stopband width, (2) minimizing the area under passband sidelobes, (3) increasing transition bandwidth.

Table 2 summarizes the results in the figures. It presents the amplitude of the peak ripple appearing adjacent to the main lobe, and the transition bandwidth between the stopband corner frequency and the passband corner frequency. To present a qualitative comparison, one can report the following points:

(1) The Blackman window has a slightly wider stopband and less sideband leakage than the Hamming and Hanning windows.

(2) The heights of the sidelobes of the Hanning window fall off more rapidly than do those of the Hamming window. Also for both of these windows the main lobes are four times as wide as the sidelobes, excepting the split sidelobes nearest the main lobe.

(3) The Blackman window also decreases the sidelobes level, and increases the width of the stopband.

(4) For the Kaiser window, the parameter β controls the sidelobe height [13]. As β increases, the sidelobe height decreases and the main lobe width increases.

5. CONCLUSION

The characteristics of an acoustic filter based on the stopband interaction of acoustic waves in periodically undulated ducts have been presented. Applying different types of taper functions to the wall undulations was found to improve the design by widening the stopband and suppressing the passband ripples. The choice of taper functions was inspired by the concept of windowing in the field of digital signal processing. The filter responses obtained in this paper were found surprisingly similar to the filter responses of windowed DSP filters having corresponding window functions as the taper functions applied to the undulations. The thesis of this work is to report that the factors used to realize a better filter response of DSP filters can be utilized as a lead in shaping the desired filter response of periodic physical filters.

REFERENCES

1. A. H. NAYFEH 1974 *Journal of the Acoustical Society of America* **56**, 768–770. Sound waves in two-dimensional ducts with sinusoidal walls.
2. A. H. NAYFEH 1975 *Journal of the Acoustical Society of America* **57**, 1036–1039. Acoustics waves in ducts with sinusoidally perturbed walls and mean flow.
3. A. H. NAYFEH and O. A. KANDIL 1978 *American Institute of Aeronautics and Astronautics Journal* **16**, 1041–1045. Propagation of waves in cylindrical hard-walled ducts with generally weak undulations.
4. A. NUSAYR 1980 *Journal of the Acoustical Society of America* **67**, 1472–1476. Propagation in rectangular ducts with sinusoidal undulations.
5. A. BOSTROM 1983 *Wave Motion* **5**, 59–67. Acoustic waves in a cylindrical duct with periodically varying cross-section.
6. L. LUNDQVIST and A. BOSTROM 1987 *Journal of Sound and Vibration* **112**, 111–124. Acoustic waves in a cylindrical duct with infinite, half-infinite, or finite wall corrugations.
7. C. E. BRADLEY 1994 *Journal of the Acoustical Society of America* **96**, 1844–1853. Time harmonic acoustic Bloch wave propagation in periodic waveguides. Part I Theory.
8. M. A. HAWWA, C. R. FULLER and R. A. BURDISO 1998 *The Journal of the Acoustical Society of America*, to appear. Stopband behavior of acoustic waves in a circular cylindrical duct with a rigid wavy wall.
9. L. R. RABINER and B. GOLD 1975 *Theory and Applications of Digital Signal Processing*. Englewood Cliffs, NJ: Prentice Hall.
10. A. V. OPPENHEIM and R. W. SCHATER 1989 *Discrete-Time Signal Processing*. Englewood Cliffs, NJ: Prentice Hall.
11. A. H. NAYFEH 1981 *Introduction to Perturbation Techniques*. New York: Wiley-Interscience.
12. O. R. ASFAR and A. M. HUSSEIN 1989 *International Journal of Numerical Methods in Engineering* **28**, 1205–1216. Numerical solution of linear two-point boundary-value problems via the fundamental matrix method.
13. J. F. KAISER 1974 *Proceedings of the 1974 IEEE International Symposium on Circuits and Systems*, 123–126. Non-recursive digital filter design using the I_0 -sinh window function.